

Supporting Information

Optically Reconfigurable Chiral Microspheres of Self-Organized Helical Superstructures with Handedness Inversion

Ling Wang,^a Dong Chen,^b Karla G. Gutierrez-Cuevas,^a Hari Krishna Bisoyi,^a Jing Fan,^{b,c} Rafael S. Zola,^d Guoqiang Li,^e Augustine M. Urbas,^f Timothy J. Bunning,^f David A. Weitz,^b and Quan Li^{*a}

^aLiquid Crystal Institute and Chemical Physics Interdisciplinary Program, Kent State University, Kent, Ohio 44242, USA; ^bSchool of Engineering and Applied Sciences, Harvard University, Cambridge, Massachusetts 02138, USA; ^cDepartment of Mechanical Engineering, The City College of New York, New York 10031, USA; ^dDepartamento de Física, Universidade Tecnológica Federal do Paraná-Apucarana, PR 86812-460, Brazil; ^eVisual and Biomedical Optic Lab, Department of Ophthalmology and Visual Science, Ohio State University, Columbus, Ohio 43212, USA; and ^fMaterials and Manufacturing Directorate, Air Force Research Laboratory, Wright-Patterson Air Force Base, Ohio 45433, USA

*Email: qli1@kent.edu (Q.L.)

Contents

- 1. Experimental materials and methods**
- 2. Synthesis and characterizations of light-driven chiral switch Azo4**
- 3. Properties of chiral switch in liquid crystals**
- 4. Fabrication and properties of cholesteric microdroplets**
- 5. References**

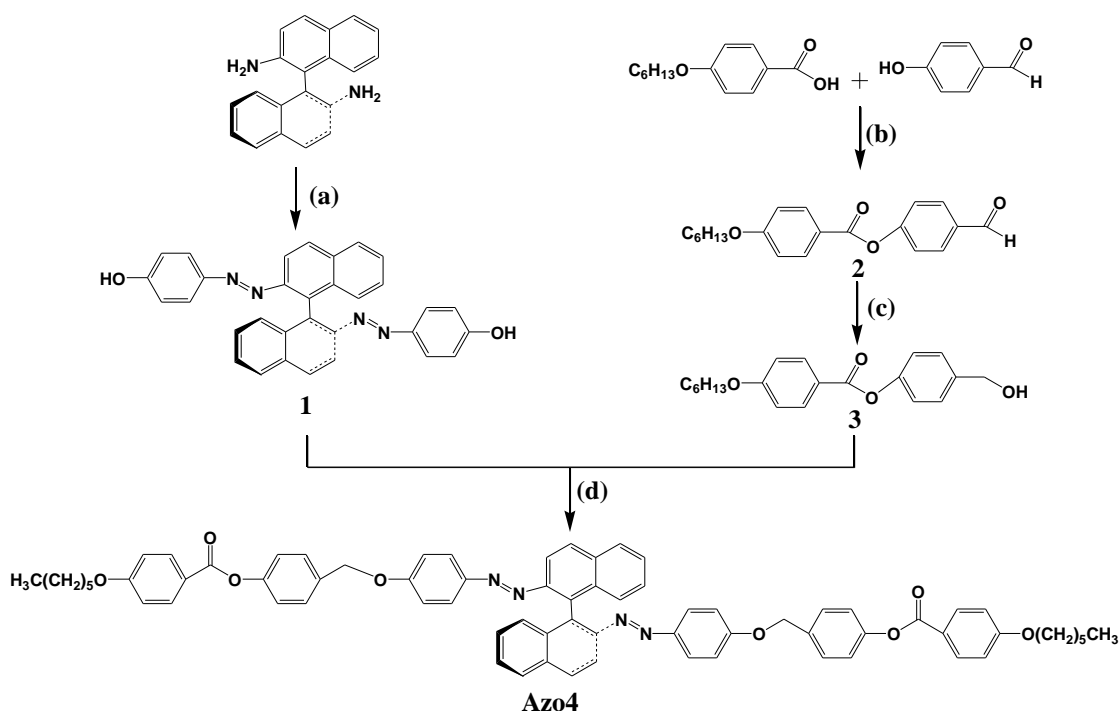
1. Experimental materials and methods

All chemicals and solvents were purchased from commercial suppliers and used without further purification. ^1H NMR (400 MHz) and ^{13}C NMR (100 MHz) spectra were recorded on a Bruker 400 MHz spectrometer using CDCl_3 as solvent at 25 °C. Chemical shifts are in δ units (ppm) with the residual solvent peak of chloroform at 7.28 ppm and 77.00 ppm for ^1H NMR and ^{13}C NMR splitting patterns are designated as follows: s, singlet; t, triplet; and tt, triplet of triplets. Column chromatography was performed using silica gel (230-400 mesh) as stationary phase. Elemental Analysis (EA) was made by Robertson Microlit Laboratories. UV-vis spectrum was taken by a Perkin Elmer Lambda 25 Spectrometer.

The commercially available liquid crystal SLC 1717 (Slichem Liquid Crystal Material Co., Ltd, $T_{N-I} = 91.8$ °C, $\Delta n = 0.22$, $\Delta\epsilon = 12.2$ at 298 K) and chiral dopant R5011 (HCCH) were used in the study. We judiciously choose the photoinensitive parter R5011 owing to its high HTP value and greater solubility in the LC meduim. These characteristics of R5011 helps to keep its doping concentration as little as possible and thus avoid phase separation problem. SLC 1717 is an eutectic mixture of LC components commercially designed for display application. Textures and disclination of liquid crystals were observed by optical microscopy using a Leitz polarizing microscope with temperature controller or Nikon polarizing microscope, reflection spectra were measured with a spectrometer in the dark. The shift in the photonic band gaps upon light irradiation was recorded using a spectrometer (USB4000, Ocean Optics). The UV and visible light irradiation was carried out with the help of Xenon light source (100 W, UVGL-58, UVP Co.) through a filter at 365 or 460 nm.

2. Synthesis of light-driven chiral switch Azo4

The light-driven chiral molecular switch **Azo4** was synthesized according to the procedure as shown in **Scheme S1**.



Scheme S1. Synthetic route of light-driven chiral molecular switch **Azo4**. Reactants and conditions: (a) i) HCl, NaNO₂, 0 °C, ii) Phenol, NaOH, 0 °C; (b) DCC, DMAP, DCM, r.t.; (c) NaBH₄, THF, 0 °C and (d) PPh₃, DIAD, THF, reflux.

Synthesis of azobenzene intermediate 1: In a round bottom flask (S)-2,2'-diamino-1,1'-binaphthyl (0.557 g, 1.9 mmol) was dissolved in a 10 mL solution of diluted HCl (1:1) and placed in an ice bath. Then, a solution of NaNO₂ (0.30 g, 4.3 mmol) in water (5 mL) was added dropwise to the cooled solution. The resulting mixture was added dropwise to an one-neck round bottom flask containing a cooled solution of phenol (0.53 g, 5.6 mmol), NaOH (0.9 g, 22.5 mmol) and water (10 mL) and reacted for 2 hours.¹ The mixture was acidified to pH=2 and filtered. The precipitated obtained, was filtrated and washed with water. After the solid was dried, the product was purified by silica column using a mixture of DCM: ethyl acetate to give a brownish orange solid. Yield: 30.2%. ¹H NMR (CDCl₃, 400 MHz) δ: 5.30 (s, 2H, Ar-OH), 6.60-6.70 (m, 4H, Ar-H), 7.20-7.30 (m, 6H, Ar-H), 7.40-7.60 (m, 4H, Ar-H), 7.95-8.00 (m, 2H, Ar-H), 8.05-8.10 (m, 2H, Ar-H), 8.15-8.20 (m, 2H, Ar-H); ¹³C NMR (CDCl₃, 100 MHz) δ: 114.66, 115.66, 124.98, 126.80, 127.16, 127.9, 128.24, 129.24, 134.39, 136.73, 147.50, 148.52 and 158.20.

Synthesis of intermediate aldehyde 2: In a round bottom flask 4-(hexyloxy)benzoic acid (1.00 g, 4.7 mmol), 4-hydroxybenzaldehyde (0.83 g, 6.79 mmol), N,N'-dicyclohexylcarbodiimide (1.01 g, 4.8 mmol) and 4-dimethylaminopyridine (0.58 g, 4.7 mmol) and 100 mL of dichloromethane were placed and mixed at room temperature for 16

hours under N₂ atmosphere. After the reaction completed, the mixture was filtered. The filtrate was rotate-evaporated to remove the DCM solvent, and the crude product obtained was purified by silica gel column using a mixture of ethyl acetate: hexane (1:4) to obtain a solid. Yield: 78.91%. ¹H NMR (CDCl₃, 400 MHz) δ: 0.93 (t, 3H, CH₃-CH₂, J=7.00 Hz), 1.30-1.60 (m, 4H, -CH₂-), 1.80-1.90 (tt, 2H, -CH₂-CH₂-O), 4.05 (t, 2H, -CH₂-O-, J=6.56 Hz), 7.00 (m, 2H, Ar-H), 7.40 (m, 2H, Ar-H), 7.95 (m, 2H, Ar-H), 8.15 (m, 2H, Ar-H), 10.05 (s, 1H, Ar-CHO); ¹³C NMR (CDCl₃, 100 MHz) δ: 14.03, 22.59, 25.66, 29.04, 31.54, 68.40, 114.45, 120.81, 122.61, 131.23, 132.44, 133.90, 155.93, 163.90, 164.26 and 190.99.

Synthesis of intermediate alcohol 3: In an ice bath, intermediate **2** (0.46 g, 1.4 mmol) and 20 mL of THF were placed and stirred. After 10 minutes, NaBH₄ (0.08 g, 2.1 mmol) was slowly added and stirred for 1 hour. Then 100 mL of ethyl acetate and a diluted solution of NH₄Cl were added. The organic phase was extracted and washed three times with water before being dried with anhydrous MgSO₄. The solvent was removed and the solid remained was purified by silica column chromatography using a mixture of ethyl acetate: hexane (1:4) to obtain a white solid.² Yield: 94.64%. ¹H NMR (CDCl₃, 400 MHz) δ: 0.95 (t, 3H, CH₃-CH₂, J=7.13 Hz), 1.38-1.53 (m, 4H, -CH₂-), 1.80-1.90 (tt, 2H, -CH₂-CH₂-O-), 4.07 (t, 2H, -CH₂-O, J=6.52 Hz), 4.73 (s, 1H, CH₂-OH) 7.00-7.05 (m, 2H, Ar-H), 7.20-7.23, 7.40-7.45 (m, 2H, Ar-H), 8.15-8.20 (m, 2H, Ar-H); ¹³C NMR (CDCl₃, 100 MHz) δ: 14.04, 22.60, 25.67, 29.08, 31.56, 64.83, 68.35, 114.31, 121.46, 122.00, 128.10, 132.30, 138.38, 150.50, 163.58 and 163.05. Elemental analysis calculated for C₂₀H₂₄O₄: C, 73.15; H, 7.37, found: C, 72.91; H, 7.50.

Synthesis of chiral molecular switch Azo4: In a two neck round bottom flask intermediate azobenzene **1** (0.52 g, 1.05 mmol), intermediate alcohol **3** (1.04, 3.16 mmol), triphenylphosphine (0.94 g, 3.58 mmol) and 100 mL of THF anhydrous were placed. The mixture was cooled by an ice bath for 20 minutes and stirred, DIAD (0.80 g, 3.9 mmol) was added dropwise and the mixture was kept under the same conditions for 20 minutes and then heated to reflux for 24 hours under constant stirring. When reaction was completed the solvent was rotate evaporated and the product was purified by column using dichloromethane as eluent. Yield: 77.10%. ¹H NMR (CDCl₃, 400 MHz) δ: 0.95 (t, 3H, CH₃-CH₂, J=7.12 Hz), 1.38-1.53 (m, 4H, -CH₂-), 1.80-1.90 (tt, 2H, -CH₂-CH₂-O-), 4.07 (t, 2H, -CH₂-O, J=6.53 Hz), 4.73 (s, 1H, CH₂-OH) 7.00-7.05 (m, 2H, Ar-H), 7.20-7.23, 7.40-7.45 (m, 2H, Ar-H), 8.15-8.20 (m, 2H, Ar-H); ¹³C NMR (CDCl₃, 100 MHz) δ: 14.04, 22.60, 25.67, 29.08, 31.56, 64.83, 68.35, 114.31, 121.46, 122.00, 128.10, 132.30, 138.38, 150.50, 163.58 and 163.05.

Elemental analysis calculated for $C_{72}H_{66}N_4O_8$: C, 77.54; H, 5.96; N, 5.02, found: C, 77.30; H, 6.17, N, 5.11.

The new chiral switch **Azo4** exhibits the expected reversible photoswitching behaviors in organic solvent. Irradiation of 50 μ M solution of (*trans, trans*)-**Azo4** in CH_2Cl_2 with 365-nm UV light resulted in the photoisomerization towards (*cis, cis*)-**Azo4**, as evidenced by a decrease in the absorbance at 355 nm and an increase of absorbance at 466 nm (**Figure S1a**). The distinct changes of CD spectra upon light illumination further gave a prominent evidence on the photoswitchable chiroptical properties of chiral molecular switch **Azo4** (**Figure S2a**). The reverse process was accomplished within 5 min upon visible light (460 nm, 30 mW/cm^2) exposure. As expected, there is no change in UV-vis absorption (**Figure S1b**) and CD spectra (**Figure S2b**) of pure **R5011** in CH_2Cl_2 upon UV irradiation. The mixed solution of 25 μ M **R5011** and 25 μ M **Azo4** in CH_2Cl_2 upon UV irradiation exhibited spectral changes corresponding to the photoresponsive attribute of **Azo4** molecular switch (**Figure S1c** and **S2c**).

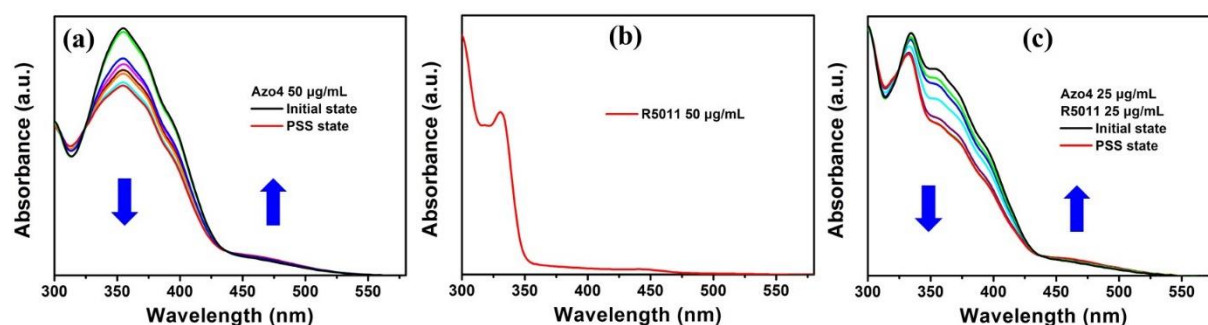


Figure S1. Changes in the UV-vis absorption spectra (a) 50 μ M **Azo4** in CH_2Cl_2 , (b) 50 μ M **R5011** in CH_2Cl_2 , (c) 25 μ M **R5011** and 25 μ M **Azo4** in CH_2Cl_2 , at room temperature in going from the initial state to photostationary state upon UV irradiation at 365 nm. Due to lack of photoswitchable moieties in **R5011**, it does not exhibit any change in its absorption spectrum upon UV irradiation.

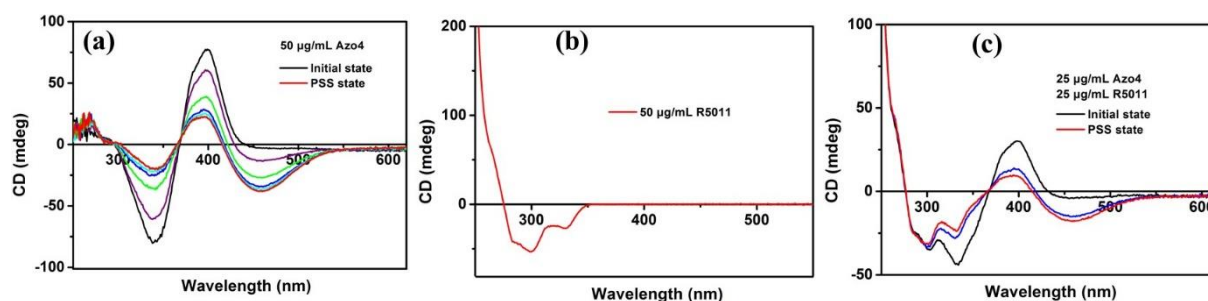


Figure S2. Changes in the CD spectra 50 μ M **Azo4** in CH_2Cl_2 , (b) 50 μ M **R5011** in CH_2Cl_2 , (c) 25 μ M **R5011** and 25 μ M **Azo4** in CH_2Cl_2 , at room temperature in going from the initial state to photostationary state upon UV irradiation at 365 nm. Due to lack of photoswitchable moieties in **R5011**, it does not exhibit any change in its CD spectrum upon UV irradiation.

3. Properties of chiral switch **Azo4** in liquid crystals

A conventional technique for pitch measurement is Grandjean-Cano wedge method.³ Such wedge cell with an opening angle θ is made by applying two differently sized spacers at each end of the cell (**Figure S3**). If the alignment of the substrates is planar (the director lies parallel to the surface) and the rubbing directions of the substrates are parallel to one another, the cholesteric LC becomes discrete. Because the value of the pitch is fixed, and the alignment is also fixed, the cholesteric LC arranges itself as depicted in **Figure S3**. This arrangement produces disclination lines between areas that contain a different number of layers. The difference in thickness between each domain must be $p/2$ in order to satisfy the alignment boundary condition. The disclination lines of the cholesteric LC in the wedge cell can be seen through a polarizing optical microscope. The pitch was determined according to the equation $p = 2R \tan \theta$, where R represents the distance between the Grandjean lines and θ is the wedge angle of wedge cells (EHC, KCRK-07, $\tan \theta = 0.0196$). The inverse of pitch proportionally increases with increase in the concentration of a chiral dopant and HTP values is $\beta = 1/(pc)$, where β is the helical twisting power, *i.e.*, the ability of the chiral dopant to twist a nematic LC, and c is the concentration of the chiral dopant.

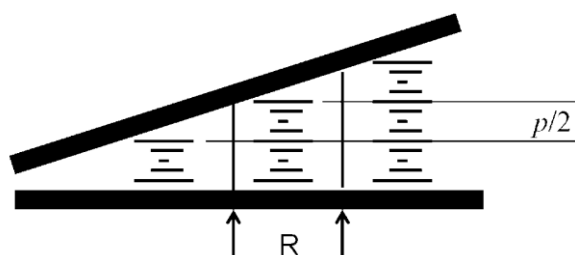


Figure S3. Schematic illustration of a Grandjean-Cano wedge cell for the pitch measurement of cholesteric LC. Disclination lines are pointed out with arrows and the thickness change between two domains is marked as $p/2$.

The chiral nematic LC was prepared by weighing appropriate amount of achiral LC host and chiral dopant into a vial followed by the addition of a few drops of dichloromethane. After evaporation of the solvent under reduced pressure, the mixture was loaded into the Grandjean-Cano wedge cell by capillary action at room temperature. The pitch was then determined by measuring the intervals of Cano's lines appearing on the surfaces of wedge-type liquid crystalline cells. Three different concentrations were used by this method for each sample, and the HTP were determined by plotting $1/p$ (μm^{-1}) against concentration of the dopant c (wt% or mol%) according to the equation $\beta = 1/(pc)$. **Figure S4** shows the HTP value change of 0.6 wt% **Azo4** in commercially available LC host SLC 1717 upon alternating UV (365 nm) or visible (460 nm) light irradiation. Moreover, the HTP value of R5011 in SLC 1717 is around $106.6 \mu\text{m}^{-1}$.

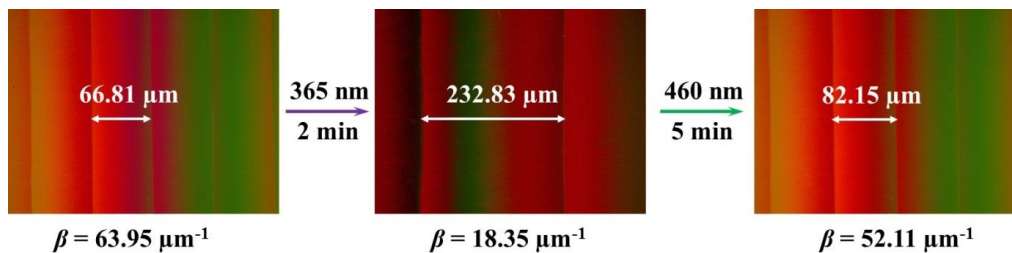


Figure S4. HTP value change of 0.6 wt% **Azo4** in commercially available LC host SLC 1717 upon UV or Vis light irradiation.

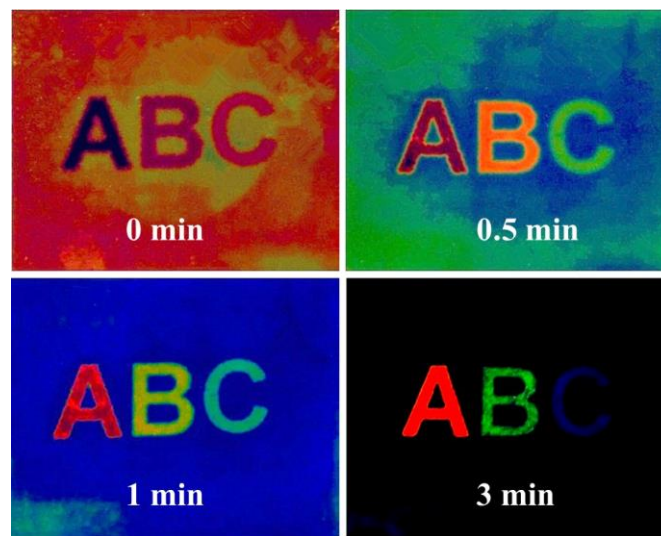


Figure S5. The real images of a 10 μm thick CLC film in a planar cell ($2.2\text{ cm}\times 2.5\text{ cm}$) filled with 8 wt% **Azo4** in SLC1717 during visible light (460 nm) irradiation. Note: the image at 0 min was obtained by 2 min UV (365 nm) irradiation of photopatterned CLC film, *i.e.*, UV PSS

When the LC mixture of 1 wt% chiral switch **Azo4** and 0.4 wt% **R5011** in SLC1717 was filled into a wedge cell and irradiated with UV light (365 nm, $15\text{ mW}/\text{cm}^2$) as shown in **Figure S6**, the Cano's lines moved outwards (0.5 min), which indicates an increase in pitch length; the lines began to disappear within 1 min, and an apparently nematic phase (infinite pitch CLC) was observed in the wedge cell as a result of the total unwinding of the induced cholesteric phase. Upon further irradiation with UV light, an oily streak texture of the CLC was observed (1.5 min), and Cano's lines were re-formed at photostationary state (PSS) within 5 min. **Figure S7** illustrates the change in handedness of 10 wt% chiral switch **Azo4** and 4 wt% **R5011** in SLC1717 upon UV irradiation (365 nm, $30\text{ mW}/\text{cm}^2$) in a 10 μm thick planar cell. At the initial state, the CLC exhibits a characteristic Grandjean texture as expected of a short-pitch CLC. After exposure to UV light, the oily streak defects of the CLC gradually disappears (0-90 s) and birefringence color of untwisted transient nematic phase with planar alignment is observed (100-120 s). Continued UV exposure of the CLCs generates the fingerprint texture which is characteristic of a long-pitch CLC (140-160 s). With

continued UV exposure, the CLC transitions once again to the Grandjean texture (180-300 s). The unique transition sequence of cholesteric \rightarrow untwisted transient nematic \rightarrow cholesteric phase ascertained the inversion of the helical handedness of the CLC. The helix of one handedness unwound, and disappeared at a critical point with infinite pitch, and then rewound through self-organization into helical superstructure of opposite twist sense.

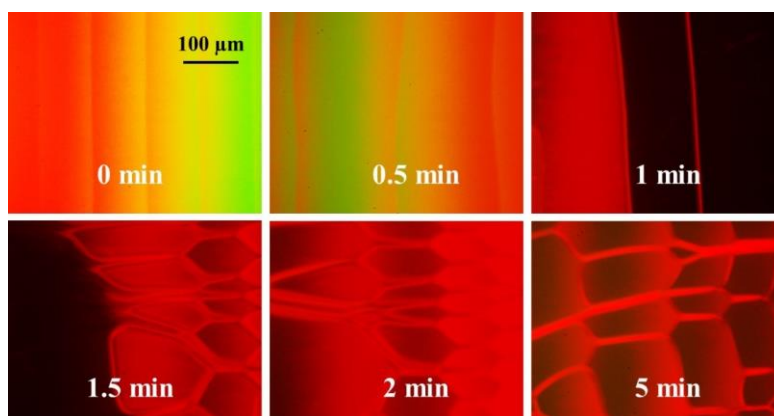


Figure S6. A change in handedness of the CLC containing 1 wt% chiral switch **Azo4** and 0.4 wt% **R5011** in SLC1717 was observed upon UV irradiation (365 nm, 30 mW/cm²) in a wedge cell.

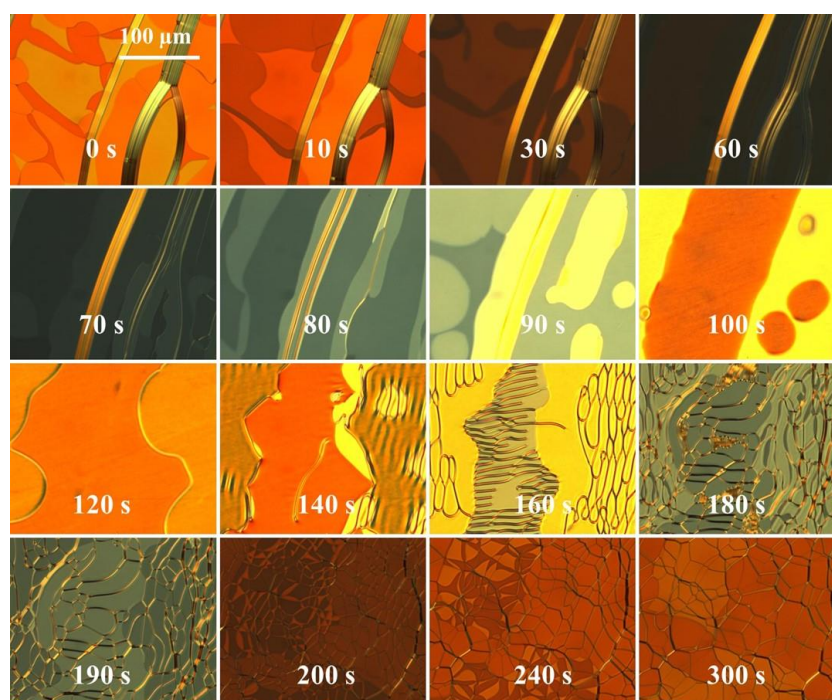


Figure S7. A change in handedness of of the CLC containing 10 wt% chiral switch **Azo4** and 4 wt% **R5011** in SLC1717 was observed upon UV irradiation (365 nm, 30 mW/cm²) in a 10 μm planar cell.

4. Fabrication and properties of cholesteric microdroplets

The microfluidic device for fabricating monodisperse CLC drops is composed of two tapered cylindrical glass capillaries coaxially assembled into a square glass capillary as shown in

Figure S8.⁴ A micropipette puller (Sutter Instrument, P-97) was used to taper the cylindrical capillaries (World Precision Instruments Inc., I.D. = 580 μm & O.D. = 1 mm) and then a microforge (Narishige, MF-830) was utilized for polishing the tip to a desired orifice size. The typical orifice diameter for inner phase injection was ~ 40 μm , and for drop collection was ~ 140 μm . Both injection and collection capillaries were treated with {2-[methoxy(polyethyleneoxy)-propyl]-9-12 trimethoxysilane (Gelest Inc.) to guarantee their hydrophilicity. The tapered capillaries were then fit into a square capillary with an inner dimension of 1.05 mm (Atlantic International Technology Inc.).

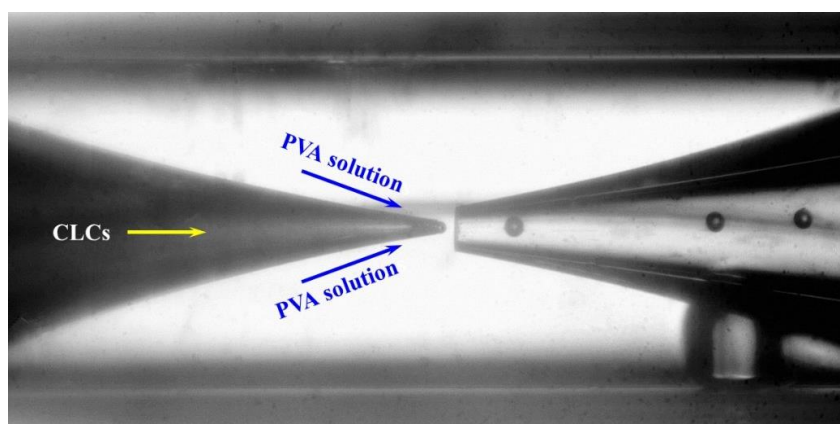


Figure S8. Fabrication of the monodisperse chiral liquid-crystalline microdroplets from the CLCs by using a glass capillary-based microfluidic device. The microdroplets are supported and surrounded by 10% PVA aqueous solution.

The flow rates of the inner and outer phases were separately controlled by using syringe pumps (Harvard PHD 2000). To decrease the viscosity of the CLC phase for a stable generation of drops, a heat gun (Wagner Spray Tech Corporation, MHT3300) was used to heat up the CLCs in the capillary right before its entering the microfluidic device above its clear point. The microfluidic experiment was conducted with a Leica DMIRB Inverted Microscope and Phantom V9 high speed camera. The emulsion droplets were sucked into a chamber consisting of two parallel glass slides by capillary force. The distance between the two slides was 125 μm , which was controlled by spacers of the specific thickness. After filled with the emulsion droplets, all the openings of the chamber were sealed by epoxy to avoid water evaporation from the continuous phase.

The light-driven structural evolution of these chiral microdroplets associated with dynamic handedness inversion is schematically illustrated in **Figure S9**. Under the parallel boundary condition, CLCs confined in the microdroplets adopt a radial orientation with the helical axes perpendicular to spherical interfaces (Figure S9a), and self-organized helicoidal

superstructures were formed as LC molecules spatially rotated along the helical axis in a clockwise or counterclockwise fashion (Figure S9b). At the initial state, the combined doping of two chiral molecules yields an overall left handedness of helical superstructures with a pitch of $\sim 4.96 \mu\text{m}$, *i.e.*, (*trans, trans*)-**Azo4** plays a dominant role in dictating handedness (Figure S9c). Upon UV irradiation, the HTP contribution from (*trans, trans*)-**Azo4** decreases significantly owing to its *trans-cis* isomerization, while the **R5011** still maintains a comparable right-handed contribution, which results in the increase of helical pitch (Figure S9d). The helix of left handedness unwinds, and untwisted transient nematic phase with infinite pitch can be observed when two opposite-handed dopants exhibit equal net HTP values (Figure S9e). Further UV irradiation leads to the rewinding of helicoidal superstructures through self-organizing into the right-handed helix (Figure S9f) accompanied by the decrease of helical pitch (Figure S9g). The observation of the bipolar configuration (Figure 9e) clearly ascertained the dynamic handedness inversion of CLCs through a transient nematic phase under UV irradiations. As theoretically predicted,^{Error! Reference source not found.} cholesteric microdroplets with degenerate planar anchoring could exhibit three (meta)stable orientational profiles, either a spiral pattern without disclination (Figure 3a), or a concentric ring pattern with line defects (Figure 3k), or a diametrical configuration with ring defects (Figure 3l). The occurrence of these characteristic patterns in our developed single dynamic system is unprecedented.

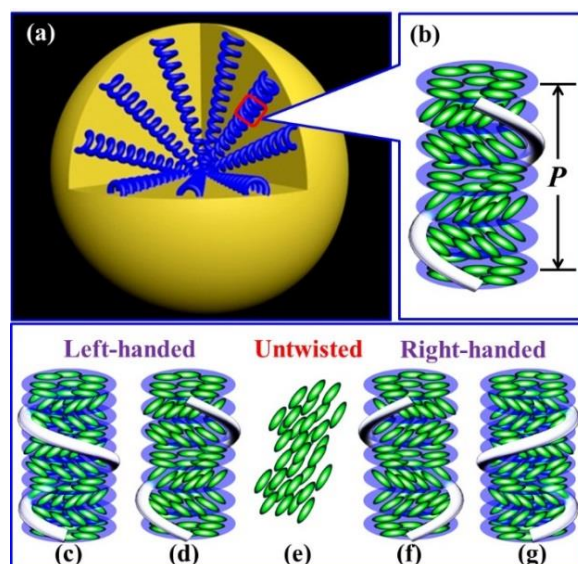


Figure S9. Schematic illustrations of dynamic handedness inversion in the monodisperse microdroplets of self-organized helical superstructures with low chirality. (a) 3D schematic configuration of a microdroplet with radial disposition of helical axes under parallel surface anchoring. (b) Helical superstructure of CLCs. (c-g) Schematics of reversible light-driven handedness inversion of CLCs.

The origin of the radial colored lines around the central spot could be attributed to lateral photonic cross-talk between the microdroplets. The mechanism behind the cross-talk is shown in **Figure S10**. According to Bragg's law of reflection, the center wavelength obeys the rule $\lambda = nP\cos\theta$, where θ is the angle between the helix axis and the light propagation direction. When $\theta = 0^\circ$, red light with wavelength nP is reflected from the droplet's core as shown in Figure S8c (red arrow). Light that hits the periphery (or inside the droplet shown by the white ray in Figure S10c) makes a non-zero incident angle with the helical axes because of the curvature, which causes an angle-dependent blue-shift from $\lambda = nP$. A CLC with defined pitch can selectively reflect light of different wavelengths depending on the angle of incidence of the light with respect to the helix axis. When $\theta = 45^\circ$, light is reflected from the left droplet to the right droplet as depicted by the blue arrow in Figure S8c. The reflected light from the first droplet is circularly polarized with the same sense as the neighbor so all the light incident from the first one is directed to the objective by the neighboring droplet. For example, the central spot is red with $\lambda = nP \approx 700$ nm at the initial state (Figure S10a), the reflected ray of this cross-talk is $nP\cos 45^\circ \approx 495$ nm for $\theta = 45^\circ$. UV irradiations lead to the increase in the helical pitch of CLCs due to the HTP decrease of photoresponsive chiral switch **Azo4**, subsequently causing the red-shift of central and peripheral reflections of microdroplets as shown in Figure S10b and Figure S10d.

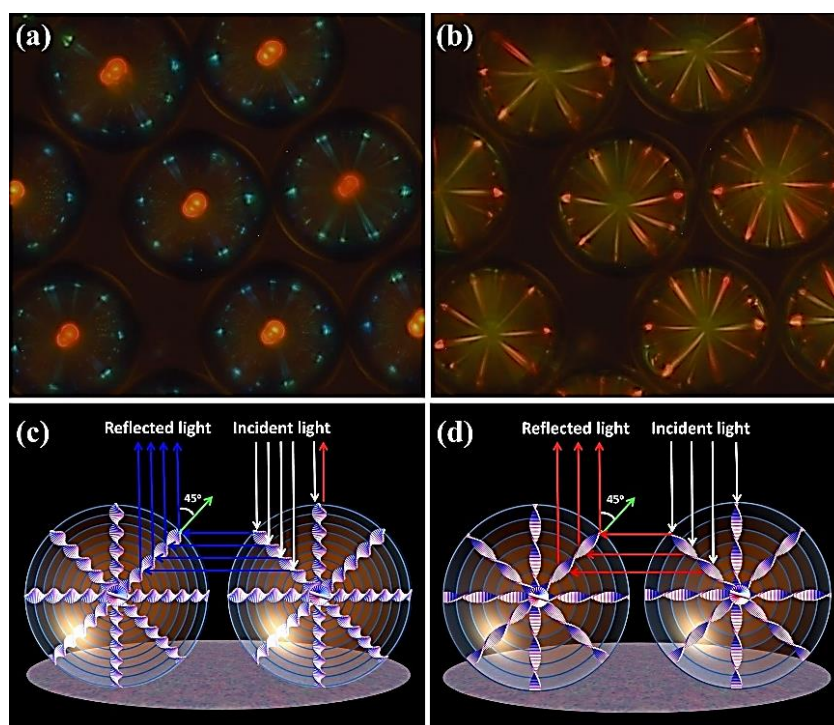


Figure S10. Light-driven tuning of photonic cross-communications between the monodisperse microdroplets. UV illumination time is 0 s (a), and 15 s (b), respectively. (c, d) Schematic mechanism of photonic cross-communications between the monodisperse CLC microdroplets with short and long pitch, respectively.

5. References

- [1] (a) Wang, L.; Dong, H.; Li, Y.; Xue, C.; Sun, L.-D.; Yan, C.-H.; Li, Q. *J. Am. Chem. Soc.*, **2014**, *136*, 4480; (b) Green, L.; Li, Y.; White, T.; Urbas, A.; Bunning, T.; Li, Q. *Org. Biomol. Chem.* **2009**, *7*, 3930.
- [2] (a) Parang, K.; Fournier, E. J.-L.; Hindsgaul, O. *Org. Lett.* **2001**, *3*, 307; (b) Zakhari, J. S.; Kinoyama, I.; Hixon, M. S.; Di Mola, A.; Globisch, D.; Janda, K. D. *Bioorg. Med. Chem.* **2011**, *19*, 6203.
- [3] Dierking, I. *Textures of Liquid Crystals*, Wiley-VCH, Weinheim, **2003**.
- [4] Fan, J.; Li, Y.; Bisoyi, H. K.; Zola, R. S.; Yang, D. K.; Bunning, T. J.; Weitz, D. A.; Li, Q. *Angew. Chem. Int. Ed.* **2015**, *54*, 2160.
- [5] (a) Y. Bouligand, F. Livolant, *J. Phys.-Paris* **1984**, *45*, 1899; (b) J. Bezić, S. Žumer, *Liq. Cryst.* **1992**, *11*, 593.